JOURNAL OF MATERIALS SCIENCE 27 (1992) 298 - 306

# Micromechanics and acoustic emission analysis of the failure process of thermoplastic composites

J. BOHSE
*Department of Materials Science, Technical College Berlin, Marktstrasse 9-12, Berlin 1134, Germany*

G. KROH
*Department of Polymer Materials Research, Technical University "Carl Schorlemmer" Leuna-Merseburg, Otto-Nuschke-Strasse, Merseburg 4200, Germany*

The finite element method (FEM) and acoustic emission technique (AE) were applied to the micromechanics analysis of the failure process of composites with thermoplastic matrix materials. FEM calculations to local stress–strain distribution and the influence of very different intermediate layer properties are interpreted with regard to microscopic failure mechanisms in composite materials. The strongly differing AE behaviour of both chalk-filled polyvinylchloride and high density polyethylene and short-glass-fibre reinforced polypropylene, polyamide, PBTP, SAN and ABS in tensile test experiments is demonstrated. Representative loading limits are derived from the nature and extent of the dominating failure mechanisms by comparison of theoretical and experimental results. The influence of critical strain, shear strength and fracture toughness properties of the modified matrix as well as the composite morphology and phase adhesion on significant deformation and failure stages is discussed. Finally some conclusions are drawn about a possible critical long-term strain of composites.

## 1. Introduction

The development of highly reliable composites requires knowledge about the influence of different structural and morphological parameters determining the microscopic deformation and fracture mechanisms which determine the strength and toughness of composites for themselves. The complexity of affecting parameters, such as matrix characteristics, nature and morphology of dispersed inclusions, as well as different phase interactions, make a complete theoretical description of effective composite behaviour nearly impossible. On this occasion the micromechanical analysis of the local composite failure process opens a way to approach the weakest volume element and to design composites with specific mechanical properties [1–6].

The development of efficient composites and a highly developed materials testing for quality valuation on the basis of evident properties such as critical long-term strain or stress and fracture toughness values, are inseparably linked..

In the last 15 years, acoustic emission (AE) analysis has crystallized into the most important technique to characterize damage propagations and mechanisms also in the case of composites with thermoplastic matrices [7–11].

Abrupt irreversible changes in the microscopic or macroscopic structure state at which elastic stored energy is released are reasons for acoustic emissions. In the case of polymers and their composites, these processes under mechanical loading are microcracking or macro-fracture and crack growth in the matrix, interface debonding, sliding of debonded regions, fibre pull-out and fibre breakage.

AE measurements permit the detection of significant damage propagation but, a priori, not an exact assignment of the emission source. Such a classification is possible only on the basis of systematic variation of structure and morphology parameters accompanied by methods to obtain deformation and fracture mechanisms directly (SEM, etc.). A new quality in the micromechanical discussion of composite failure is attainable by the combination of model calculations and AE results [6, 12–16].

## 2. Model calculations of microscopic stress–strain distribution

The combination of a soft matrix with a hard inclusion will result in a complicated structure- and morphology-dependent stress–strain state in microranges also under macroscopic uniaxial loading conditions. Decisive for the first stage of damage process and the extension of local plastic matrix deformations in composites are the size, spatial distribution and kind of stress or strain concentrations which depend on the inclusion morphology and external loading, and the



0022–2461/92 $03.00 + .12 

nature of the plastic matrix instability in a specific local stress–strain field.

The included phase influences the start and bulk more strongly than the nature of local deformation and fracture mechanisms in the polymer matrix. The latter depends on the modified matrix itself. Under strong phase interactions or overcritical filler concentrations, a change in failure mechanism of the composite matrix is possible.

Model calculations of local strains and stresses were based on a generalized plane strain finite element analysis of a typical repeating composite unit volume. With this method it was possible to calculate the influence of essential geometrical and structural composite parameters, such as matrix and inclusion properties, volume fraction and aspect ratio of inclusions, and phase adhesion and respective behaviour of interphases.

"Hybrid" finite elements were used to obtain more accurate information, especially about the stress distribution at the inclusion–matrix interface [17]. In the model calculations, different adhesion conditions were taken into account by thin interphases with realistic dimensions and properties. The validity of the calculations is restricted to linear visco-elastic deformation behaviour of polymeric areas. In the result of model analysis local distributions of dilatational strain, normal stress and shear stress components in the inclusion and matrix, as well as the interface region, are given. With regard to a critical strain for microscopic composite failure by micro-hole or micro-crack formation, the comparative strain $\varepsilon_v$, for a plane strain state was determined to evaluate local multiaxial loading conditions. From the comparative strain and model composite strain, $\varepsilon_{x0}$, a strain raising factor

$$\alpha_\varepsilon = \frac{\varepsilon_v}{\varepsilon_{x0}} \tag{1}$$

results. Figs 1 and 2 demonstrate representative results for local stress–strain distribution and their change with very different interphase properties in the case of a model composite with unidirectional fibre orientation. As shown in the figures, the maximum values and positions of individual stress components are morphologically dependent [15, 17, 18]. In the

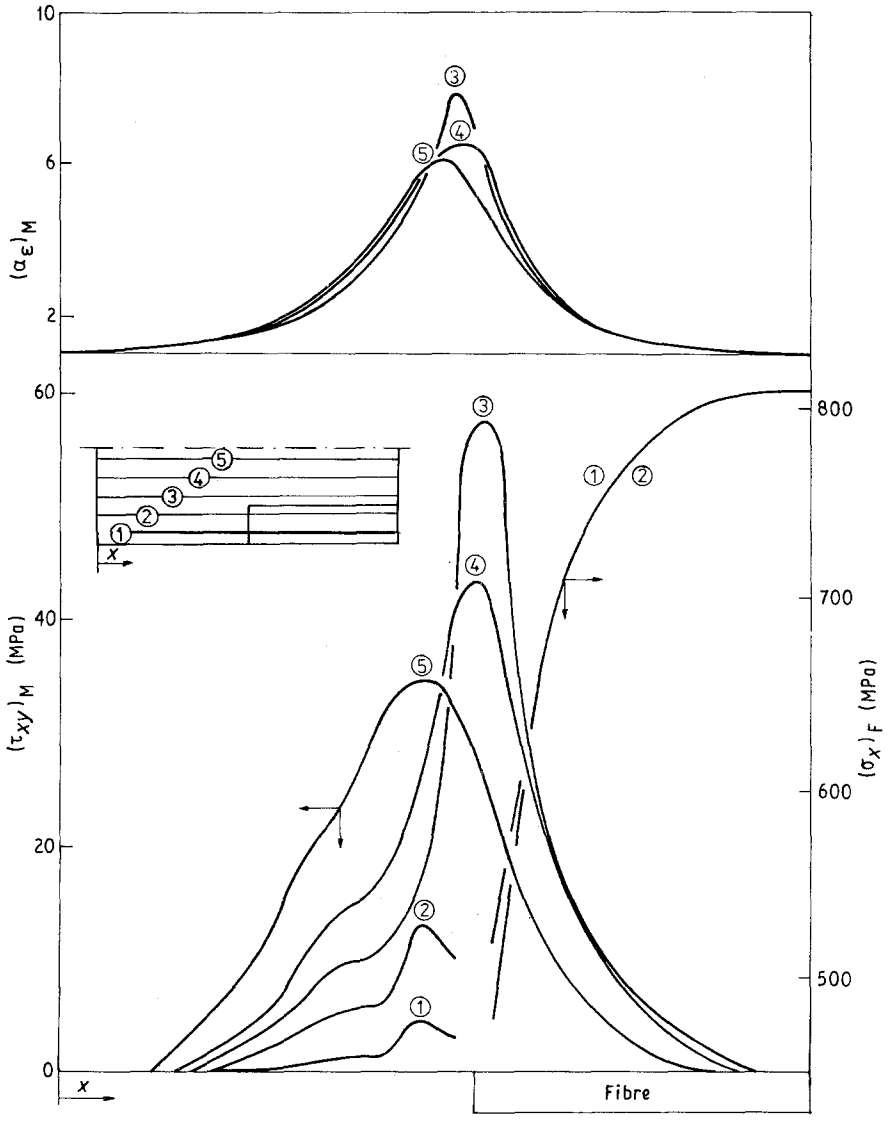


*Figure 1* Strain raising and shear stress distribution in the composite matrix $(\alpha_\varepsilon, \tau_{xy})_M$ and distribution of the main normal stress in the fibre $(\sigma_x)_F$: PP/GF composite (15 vol % GF; $L/D = 31.5$); composite strain $\varepsilon_{xo} = 1\%$ (model strain).

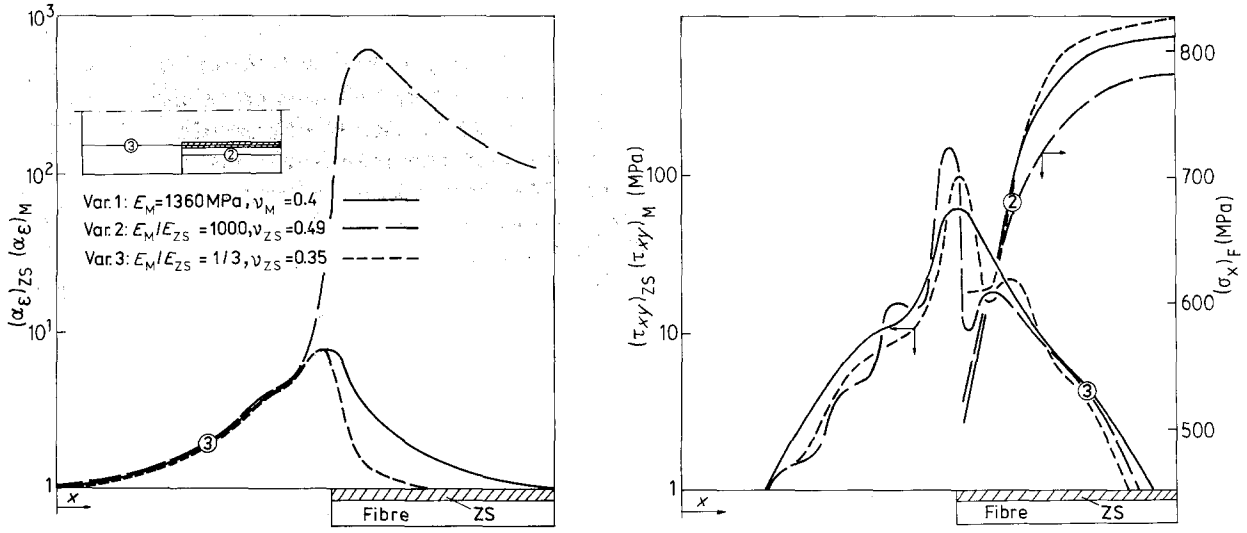


*Figure 2* Influence of interphase (ZS) on local stress–strain distribution: PP/GF composites without (Var. 1) and with interphases (Var. 2 and 3); (15 vol % GF; $L/D$ = 31.5); thickness of interphase layer = 10 nm, composite strain $\varepsilon_{x_0}$ = 1%.

case of particulate-filled composites assuming "perfect" adhesion, the maximum radial normal stress acts at the poles (angle to macroscopic tensile direction is 0°) while the maximum shear stress is found at an angle of about 45°. All matrix maxima in short-fibre-reinforced composites are located at the fibre ends. The presence of interphases changes the position and height of local stress and strain distributions. Volume elements with strain or shear stress peaks can be considered as weakest points for the beginning of damage. Mechanical behaviour of the interphases (quality of phase adhesion) is of great importance in the process of energy dissipation. A failure of interfacial regions is to be expected if:

(i) the stored deformation energy induces debonding in consequence of poor phase adhesion;

(ii) the shear stress level at the interphase obtains the shear strength;

(iii) the strain raising initiates micro-hole or crack formation at a critical strain level (strong phase interactions and hydrostatic stress states restrict shear yielding); or

(iv) the critical strain of craze formation in crazing composite matrices, is exceeded.

## 3. Acoustic emission analysis of the failure process

Acoustic emission (AE) during tensile tests was recorded and analysed using a Brüel and Kjaer system. Tensile tests were carried out at constant elongation speeds of $v_T$ = 10 mm min$^{-1}$ (particle composites) and $v_T$ = 2 mm min$^{-1}$ (fibre composites). Fig. 3a–c show very different AE activities and distributions of peak amplitude for diverse composites. Here the cumulative pulse sum is a measure of the damage accumulation. The peak amplitude of AE events is correlated with the energy release and gives a clue to the primary source of acoustic emission. Polyvinyl chloride (PVC), Fig. 3a, shows shear-band deformation accompanied by the formation of micro-holes of about 0.25–7 μm diameter. The diameter distribution of used chalk filler also corresponds with this range. Therefore, the distribution width of peak amplitudes generated by particles such as composites is similar to the non-filled matrix. Larger deviations, especially in the distribution itself, are observed when a critical filler volume causes a macroscopic ductile-to-brittle transition. This became apparent in the rupture strain falling below the level of the non-filled matrix material. At a smaller filler content than the critical one, the increase in the pulse sum indicates a multiplication of local instabilities. Hence, the raising rupture strain of particulate-filled PVC is based on the initiation of additional micro-shear bands on the particle–matrix debonding. The monitored AE spectrum of high-density polyethylene (HDPE), Fig. 3b, proves that micro-hole formation in amorphous regions takes place before the macroscopic necking process occurs. According to SEM investigations of fracture surfaces, the void diameter amounts to more than some 10 nm. The inclusion of chalk particles will result in a creation of more and essentially larger micro-holes connected with phase debonding. Dramatic changes in the distribution of peak amplitudes were observed. A marked localization of the fibrillization processes in highly stressed matrix layers was found by means of TEM investigations. Strongly reduced macroscopic rupture strains at a low particle content are the result. The damage behaviour of short-fibre-reinforced thermoplastics is also strongly influenced by the matrix polymer (Fig. 3c). Here, the interphase behaviour is of greater importance than in particulate-filled composites. The composite polypropylene (PP)/GF (1) did not contain a coupling agent. In the case of PP/GF (2) a coupling agent of optimum concentration was applied. Higher phase interactions cause a brittleness of composite with a proportion-exceeding decrease of the AE pulse sum. From the example of polyamide (PA)/GF composites, a significant influence of matrix brittleness is represented (PA/GF (1)–moist, PA/GF (2)–dried, PA/GF (3)–condensed). By means of

acoustic emission, individual deformation levels can be indicated where failure mechanisms change in nature and/or extension significantly (Fig. 4). By means of a distinct AE signature in connection with results of model calculation, the following representative loading limits can be distinguished: see Table I. AE activity expresses the essential difference in micromechanical damage behaviour between particle-filled and fibre-reinforced composites. Spherical as well as fibre-like inclusions release additional damage inside the composite matrix, respectively, by inclusion-matrix debonding, which reduces the critical composite strain.

Based on their shape, fibres are more efficient than spherical inclusions here.

In particle composites the following damage behaviour is determined by deformation and fracture processes of the modified matrix only. Fibre-like

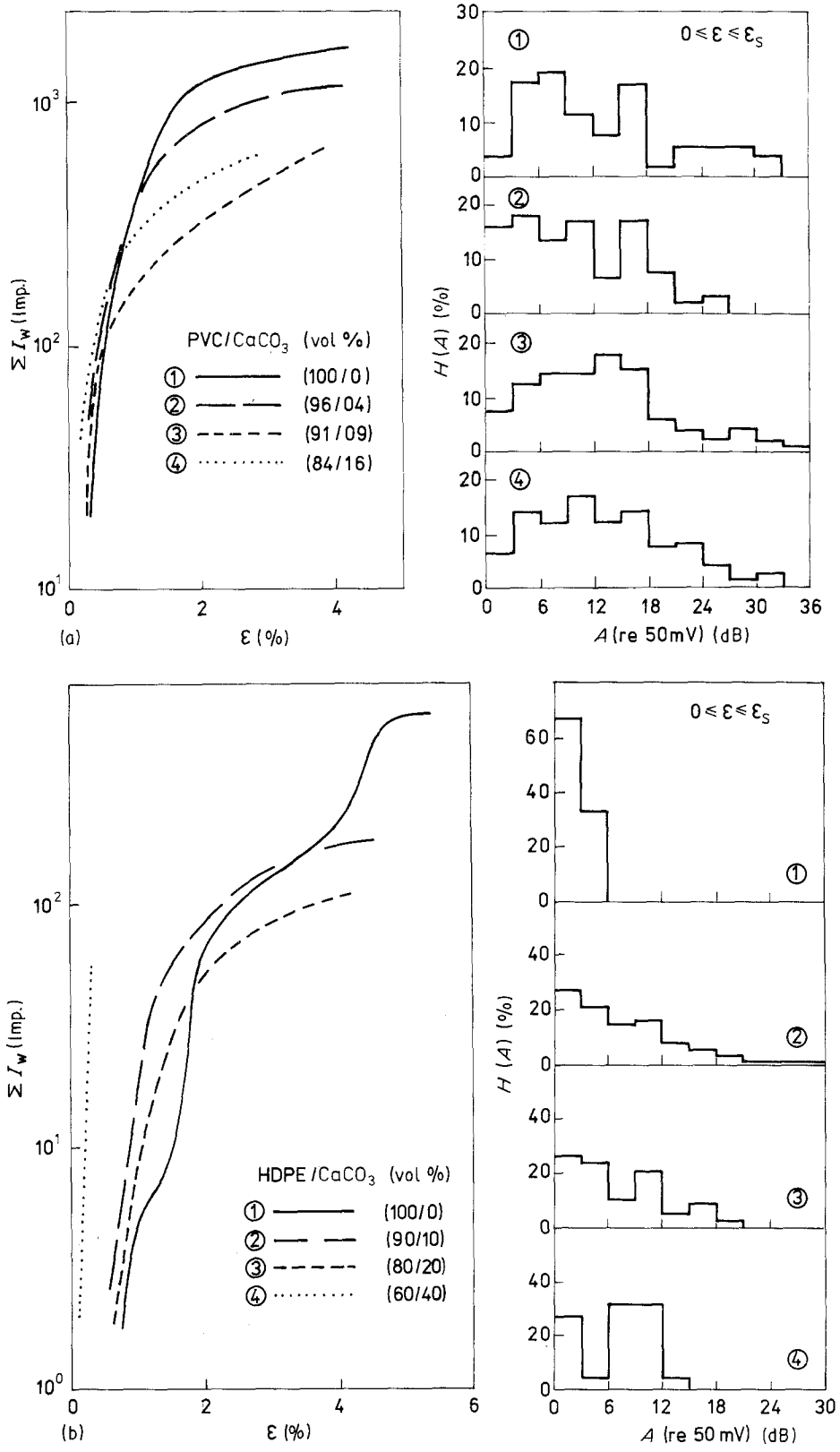


*Figure 3* Strain dependence of cumulative AE activity and total amplitude distribution of AE signals for chalk-filled thermoplastics (up to composite yield stress) and glass fibre-reinforced thermoplastics (up to ultimate composite fracture).

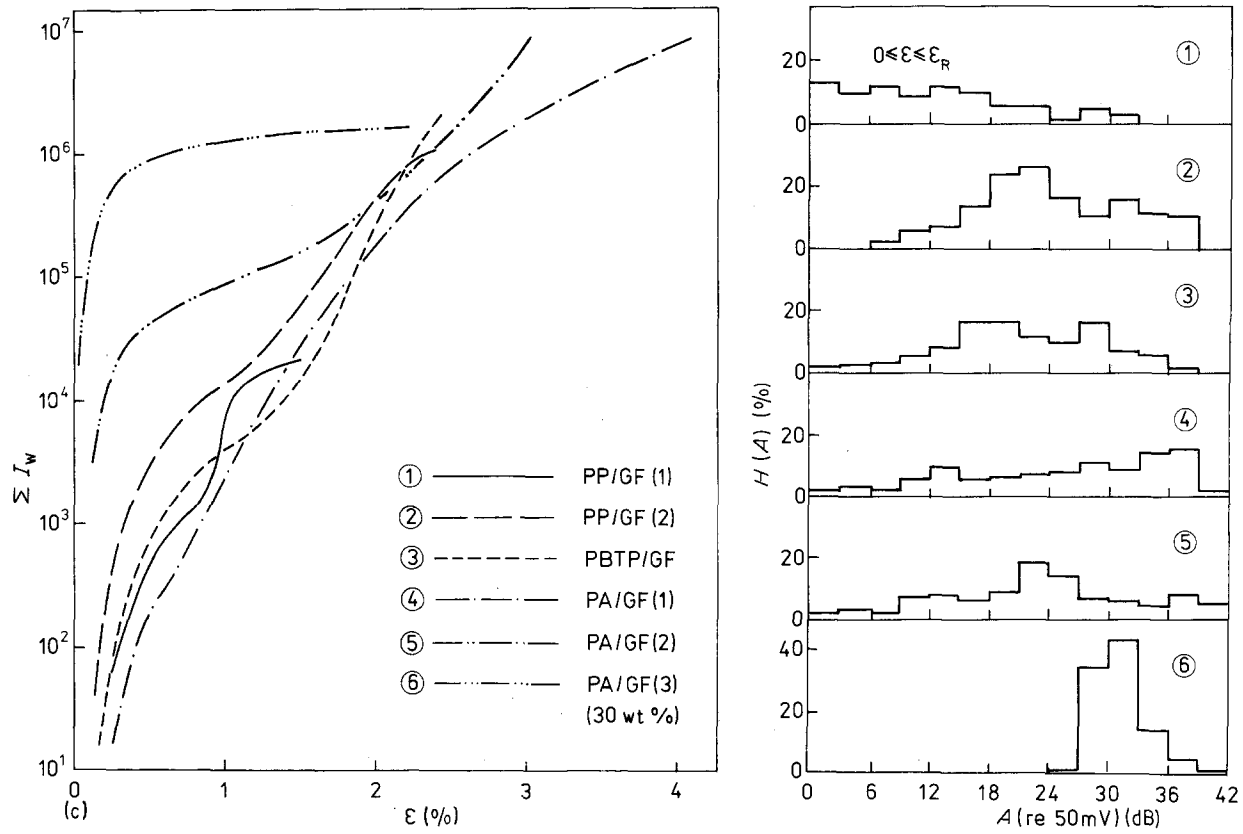


*Figure 3* Continued.

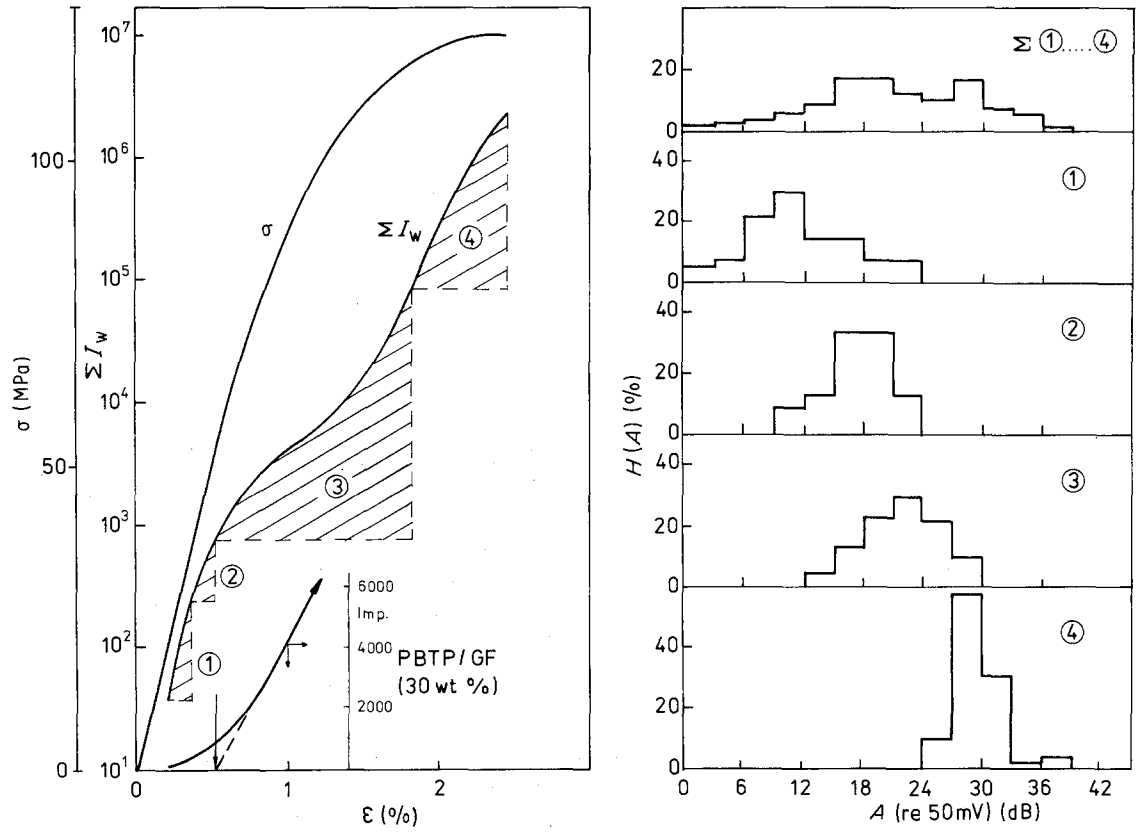


*Figure 4* AE characteristic of significant deformation states in the case of glass fibre-reinforced PBTP.

inclusions, however, stabilize the micro-crack network by the occurrence of further mechanisms of energy dissipation at the interface, such as sliding of debonded regions, fibre pull-out or fibre fracture, and they increase the ultimate composite strength. The AE behaviour of short-fibre-reinforced thermoplastics detect the mechanisms by high pulse sums and events with higher energies. Under very good adhesion

TABLE I Loading limits for the initiation of characteristic deformation stages and damage mechanisms of thermoplastic composites

| $\varepsilon_{ci}/\sigma_{ci}$ | AE characteristic | Damage mechanisms |
|---|---|---|
| *First stage* | | In areas of local loading maxima: |
| $\varepsilon_{c1}/\sigma_{c1}$ | AE begin | (i) debonding at the interface (weak phase adhesion) |
| $\varepsilon_{c2}/\sigma_{c2}$ | First relative maximum of pulse rate ($A > 20$ dB) | (ii) first damage of the interfacial region or matrix (micro-hole formation) |
| *Second stage* | | Composite damage in large matrix areas by: |
| $\varepsilon_{c3}/\sigma_{c3}$ | (a) Decreasing emission in ductile composites or at weak adhesion (existence of a macroscopic yield point) | (i) macroscopic shear flow owing to yielding of matrix bridges<br>(ii) continued inclusion–matrix debonding<br>(iii) formation of micro-shear bands |
| | (b) Strongly progressive increase of emissions at brittle matrix or good adhesion | (iv) crazing<br>(v) micro-crack formation<br>(vi) stable micro-crack growth<br>(vii) fibre sliding |
| *Third stage* | | |
| $\varepsilon_{c4}/\sigma_{c4}$ | Occurrence of signals with higher energy release in fibre composites ($A > 30$ dB) | Coalescence of micro-cracks<br>Formation of macro-fracture surface (under fibre pull-out) |
| | ($A > 40$ dB) | (Fibre breaking) |

conditions the stored deformation energy can induce fracture of overcritical long fibres. Particle fracture as a dissipation mechanism in thermoplastic composites can be excluded.

## 4. Morphology and microscopic failure mechanisms

The comparison between theoretical and experimental failure analysis permits the identification of probable mechanisms as a primary source of acoustic emissions. The comparison also gives information about the nature of interphase failure. This is deduced from theoretically calculated comparisons of strain or shear stress components in the matrix near the interface. These calculations are based on composite loads at the onset of micro-failure processes detected by means of acoustic emission. By means of the correspondence between a comparison of theoretical and experimental data in Fig. 5, the assumption is checked whether damage at the first deformation stage is a consequence of a "medium" strain raising in the matrix bulk region. Obviously the above assumption is incorrect in such composites which possess matrices with craze deformation (PS, SAN, ABS) or when the matrix failure changes from a shear mechanism in a craze-like mechanism at higher filled composites (e.g. chalk-filled HDPE with chalk contents $> 20$ vol %). As expected in the case of the craze mechanism, the absolute strain peak at the interface induces the first composite damage. Add to this that the fibre orientation in injection moulded specimens diverges from perfect unidirectional position, and the fibre distribution is irregular. However, the model with unidirectional short-fibre orientation in the loading direction describes the morphology of the by far greatest section in the specimen and submits the lowest limit of critical composite strain. The nature of the local composite failure at the first deformation stage can be derived from results of a model calculation by the application of critical composite strains from AE analysis (Table II). A valuation of phase interactions on the basis of local composite damage is problematic in this damage state. Different adhesion qualities will have a significant effect only in the case of higher deformations in the process of micro-crack growth. A theoretical description of the second and third deformation stage requires a fracture mechanics analysis of microscopic composite failure. It presupposes a knowledge of fracture toughness data of the matrix and interphase against stable crack initiation and crack growth, as well as unstable crack initiation. At present, the experimental determination of effective values for interphase fracture toughness is most difficult [2, 19, 20]. Fig. 6 indicates such a relationship between the onset of the second damage stage and the stable crack initiation toughness of the composite matrix.

This correlation confirms the assumption that relevant parameters relating to loading limit ($\varepsilon_{c3}/\sigma_{c3}$) in addition to composite morphology are stable crack initiation resistances of polymer regions.

In the theoretical analysis, however, interactions between neighbouring micro-cracks, as well as structural matrix modifications, were neglected for the first approximation. The value scattering points to this circumstance. In the case of crazing matrices (ABS, SAN) the loading limit $\sigma_{c3}$ at fibre composites is not connected with a micro-crack initiation but with the craze formation obviously.

The critical micro-crack density (critical filler content) for a ductile-to-brittle transition of matrix fracture is reached, if the crack distance drops under a critical value, $\lambda^*$

$$\lambda^* \sim 2\beta\left(\frac{J_{Ic}E}{\sigma_c^2}\right) \quad (2)$$

where $\lambda$ is the mean particle distance, $\beta$ is a mechanism-dependent factor $\leqslant \pi/8$, $J_{Ic}$ is the critical $J$-integral, $E$ is the Young's modulus and $\sigma_c$ is the stress for micro-hole formation of the polymer matrix.

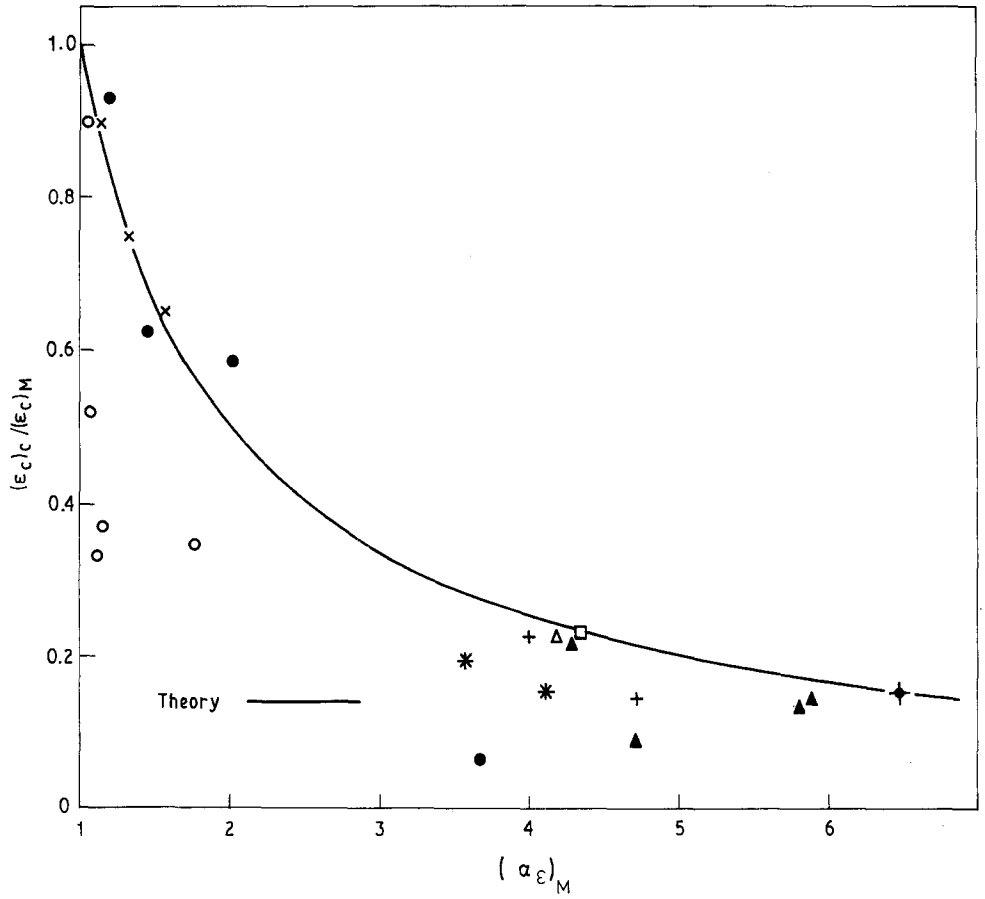


*Figure 5* Relationship between structure and morphology dependent "medium" strain raising $(\alpha_\varepsilon)_M$ in the matrix bulk (Section 5 in Fig. 1) and relative critical composite strain. (●) PE, (○) PS, (×) PVC, with $CaCO_3$; (◆) PE, (▲) PP, (□) PA, (+) ABS, (*) SAN, (△) PBTP, with GF.

TABLE II Results of model calculations in connection with experimental data of AE for composites with 30 wt % inclusions, and conclusions upon the nature of interphase failure in real composites (model calculations on the base of experimental composite strain $\varepsilon_{c2}$)

| Composite | Model | | AE | | AE/Model | | | | Failure of interphase region |
|---|---|---|---|---|---|---|---|---|---|
| | $(\varepsilon_c)_C$ (%) | $(\sigma_c)_C$ (MPa) | $\varepsilon_{c2}$ (%) | $\tau_{c2}$ (MPa) | $(\tau_{xy})_{ZS}$ (MPa) | $(\varepsilon_v)_{ZS}$ (%) | $\tau_M^0$ (MPa) | $(\varepsilon_c)_M$ (%) | |
| PE/$CaCO_3$ | 1.20 | 18 | 1.50 | 17 | 18 | 1.9 | 18 | 2.4 | Shear instability |
| PVC/$CaCO_3$ | 0.36 | 14 | 0.45 | 17 | 38 | 1.4 | 36 | 0.8 | Shear instability |
| PS/$CaCO_3$ | 0.13 | 6 | 0.10 | 4 | 6 | 0.2 | (40) | 0.3 | Crazing |
| SAN/GF | 0.24 | 25 | 0.15 | 15 | 10 | 0.6 | (50) | 1.0 | Crazing |
| ABS/GF | 0.29 | 21 | 0.19 | 15 | 12 | 0.8 | (24) | 1.3 | Crazing |
| PP/GF | 0.39 | 27 | 0.26 | 19 | 15 | 2.4 | 20 | 2.3 | Shear instability/ micro-crack formation |
| PBTP/GF | 0.43 | 40 | 0.40 | 37 | 23 | 2.0 | 37 | 1.8 | Micro-crack formation |
| PA/GF | 0.46 | 41 | 0.43 | 38 | 22 | 2.2 | 39 | 2.0 | Micro-crack formation |

$(\varepsilon_c)_C/(\sigma_c)_C$: critical composite strain/stress from model calculations for the criteria that a "medium" $\varepsilon_v$ in the matrix bulk exceed $(\varepsilon_c)_M$.
$(\tau_{xy})_{ZS}/(\varepsilon_v)_{ZS}$: maximum values of shear stress/comparative strain at the interphase region (ZS).
$\tau_M^0$: shear strength of the matrix.
$(\varepsilon_c)_M$: critical strain of unfilled matrix for the initiation of micro-hole formation or crazing (data from AE measurements).

On the basis of experimental data for particulate-filled PVC with a critical filler volume $\phi^* = 0.05$ (particle diameter 2 μm), the following $\lambda^*$ values for static loading conditions and a crack size of 2 μm were calculated: 2.4 μm (PVC), 9.2 μm (HDPE) and 1.2 μm (PS).

A complicated damage state already exists at the beginning of the third deformation stage. The toughness behaviour of polymer regions against stable crack growth and their unstable crack initiation toughness are considered to be relevant fracture mechanics values for the amount of energy dissipated at this loading level.

The above discussions leave open to question which of the loading limits must not be exceeded in order to guarantee a long life-time. Investigations of relaxation and retardation behaviour of the composites under application of AE, lead to the conclusion that a safe critical long-term strain should be in the range of $\varepsilon_{c2} \leqslant (\varepsilon_c)_C \leqslant \varepsilon_{c3}$ [11, 16]. This result is in agreement with the long-term tests of Menges *et al.* [21]. It is essential that the long-term relaxation behaviour of

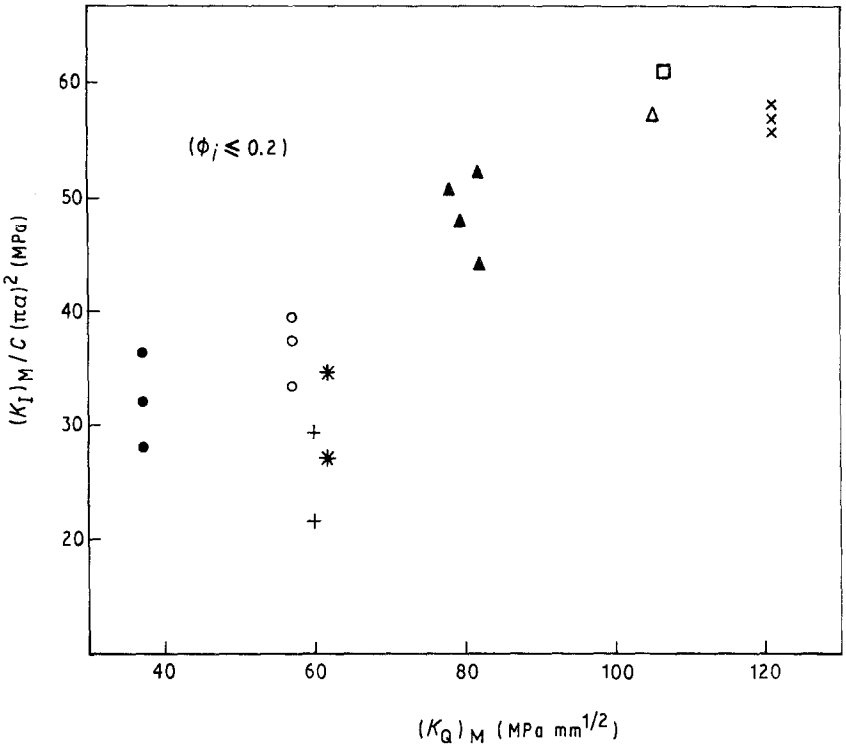


*Figure 6* Connection between theoretical stress intensity factor in the composite matrix $(K_I)_M$ at the composite stress $\sigma_{c3}$ (respectively $R_e$ or $R_m$ at chalk fillers) and critical matrix values $(K_Q)_M$ for crack initiation. (●) PE, (×) PVC, (○) PS, with $CaCO_3$; (▲) PP, (□) PA, (△) PBTP, (+) ABS, (*) SAN, with GF.

crack-affected polymer areas is of decisive importance for the long-term strength of particulate-filled and short-fibre-reinforced thermoplastics. The existence of interphases improves the strength and toughness of composites the stronger values, the more low-energetic damage (absolute and relative) being favoured in the direction of a maximum shear band or craze multiplication. The effectiveness of phase adhesion of interphases for a high long-term stability and reliability of composites, results decisively from the success in obtaining a rest life-time after initiation of the damage process, which is as high as possible. For this reason it must contribute, together with a high fracture toughness, to limiting the size of the arising micro-cracks and to hindering crack growth.

Taking these processes into account, the critical long-term strength can be extrapolated theoretically with the help of continuum damage mechanics [22].

## 5. Conclusions

1. The micromechanical analysis of macroscopic deformation behaviour of composites opens the possibility to determine long-term strains or stresses from the local damage state and to recognize structurally or morphologically weak areas.

2. The acoustic emission analysis detects the damage process as well as local failure mechanisms in composites in a highly sensitive manner. Therefore, this technique is suitable to elucidate real structural and morphological conditions.

3. The deformation process of thermoplastic composites can be classified by means of AE in connection with results of theoretical stress–strain calculations into three significant deformation stages characterized by different dominating damage mechanisms.

4. Critical composite strains and stresses for initiation of each deformation stage can be attributed theoretically to the local strain-raising factor, the shear stress level or the stress intensity factor depending on structural and morphological composite parameters. In practice they correlate with (i) critical strains or shear strength, and (ii) fracture toughness values faced with stable crack initiation and crack growth, as well as unstable crack initiation of the interface and modified composite matrix.

5. By comparing model and experimental results, it is possible to analyse the nature of interphase failure and to obtain quantitative results about the phase adhesion.

6. The composite strain where stable micro-crack initiation beings should be considered to be the limiting value of critical long-term strain.

## References

1. M. E. J. DEKKERS and D. HEIKENS, in "Composites Interfaces", edited by H. Ishida and J. L. Koenig (Elsevier Science, New York, 1986) p. 161.
2. M. R. PIGGOTT, A. SANADI, P. S. CHUA and D. ANDISON, *ibid.*, p. 109.
3. A. C. MOLONEY, H. H. KAUSCH, T. KAISER and H. R. BEER, *J. Mater Sci.* **22** (1987) 381.
4. B. LAUKE and B. SCHULTRICH, *Fibre Sci. Technol.* **19** (1983) 111.
5. H. ISHIKAWA, T.-W. CHOU and M. TAYA, *J. Mater. Sci.* **17** (1982) 832.
6. M. TAYA and T.-W. CHOU, *ibid.* **17** (1982) 2801.
7. R. BARDENHEIER and J. WOLTERS, in "Proceedings of 'Verstaerkte Plaste '84'", Berlin, FRG (1984) D8.

8. *Idem.*, in "Proceedings of 'Verstaerkte Plaste '86'", Dresden, FRG (1986) B8.
9. J. WOLTERS and G. MENNIG, *Angew. Makromol. Chem.* **125** (1984) 103.
10. J. YUAN, A. HILTNER and E. BAER, *Polym. Compos.* **7** (1986) 26.
11. C. BIEROEGEL, K. BARTNIG and J. BOHSE, in "Proceedings of 'Verstaerkte Plaste '88'", Berlin, FRG (1988) 7.4.
12. J. BOHSE, K. BARTNIG and C. BIEROEGEL, *ibid.* 7.9.
13. N. SATO, T. KURAUCHI, S. SATO and O. KAMIGATO, *J. Mater. Sci.* **19** (1984) 1145.
14. G. LEPS, J. BOHSE and M. MAY, *NDT Int.* **19** (1986) 387.
15. J. BOHSE and G. KROH, *Plaste Kautschuk* **34** (1987) 376.
16. J. BOHSE, D.Sc. techn. thesis, TH Leuna-Merseburg (1989).
17. G. KROH and J. BOHSE, *Plaste Kautschuk* **33** (1986) 110.
18. S. VOELLMAR and W. POMPE, *ibid.* **25** (1978) 78.
19. Y. W. MAI and F. CASTINO, *J. Mater. Sci. Lett.* **4** (1985) 505.
20. B. MILLER, P. MURI and L. REBENFELD, *Compos. Sci. Technol.* **28** (1987) 17.
21. G. MENGES, H. SCHLUETER and R. JONAS, "Forschungsberichte des Landes Nordrhein-Westfalen", No. 2892 (Westdeutscher Verlag, 1979) Tables 6.2 and 6.3.
22. J. LEMAITRE and J. DUFAILLY, *Engng Fract. Mech.* **28** (1987) 643.

*Received 6 March 1990*
*and accepted 25 March 1991*